Synthesis, photophysical characterization, and integration of two-photon-responsive fluorophores in mesoporous organosilica nanoparticles for biological imaging use

Nicolas Bondon, Nicolas Richy, Lamiaa M.A. Ali, Denis Durand, Magali Gary-Bobo, Yann Molard, Grégory Taupier, Frédéric Paul, Nadir Bettache, Jean-Olivier Durand, et al.

Synthesis, Photophysical Characterization, and Integration of Two-Photon-Responsive Fluorophores in Mesoporous Organosilica Nanoparticles for Biological Imaging Use

Nicolas Bondon [a, b, *], Nicolas Richy [b], Lamiaa M. A. Ali [c, d], Denis Durand [c], Magali Gary-Bobo [c], Yann Molard [b], Grégory Taupier [b], Frédéric Paul [b], Nadir Bettache [c], Jean-Olivier Durand [a], Christophe Nguyen [c], Clarence Charnay [a, *] and Olivier Mongin [b, *]

[a] ICGM, University of Montpellier, UMR-CNRS 5253, 34293 Montpellier, France

[b] Univ Rennes, CNRS, ISCR (Institut des Sciences Chimiques de Rennes) - UMR 6226, ScanMAT – UAR 2025, F-35000 Rennes, France

[c] IBMM, University of Montpellier, UMR-CNRS 5247, 34293 Montpellier, France

[d] Department of Biochemistry, Medical Research Institute, Alexandria University, Alexandria 21561, Egypt

* Corresponding authors: nicolas.bondon@outlook.com, olivier.mongin@univ-rennes1.fr, clarence.charnay@umontpellier.fr

ABSTRACT

We report the synthesis of new graftable three-branched octupolar fluorophores (F and F2), based on a triphenylamine core connected to electron-withdrawing sulfone-based peripheral groups through one or two π-conjugated phenylene-vinylene linkers. Their two-photon absorption (TPA), solvatochromism and photoluminescence properties were investigated to derive structure-property relationships. Notably, the chromophores presented TPA bands in the biological window (700-900 nm) and high TPA cross-sections at peak of 810 GM for F and F2. Then, after silylation, fluorophore F was further covalently integrated within the sol-gel synthesis of different periodic mesoporous organosilica nanoparticles (PMO NPs). Transmission electronic microscopy imaging revealed the formation of spherical NPs with good monodispersity in size, as confirmed by dynamic light scattering measurements. The obtained fluorophore-based nanoplatforms were shown to be biocompatible *in vitro* and demonstrated a good potential for two-photon imaging in cancer cells using two-photon excited fluorescence microscopy.

1. Introduction

The design of molecular chromophores possessing enhanced two-photon absorption (TPA) properties has been extensively studied in the past few years.[1-6] TPA presents several advantages for biomedical applications, such as excitation with high selectivity levels in biological environment and photodamage reduction by the use of lower excitation intensities.[7]

Among the different families of dyes, organic octupolar chromophores possessing non-centrosymmetric structure can be attractive for their multiphoton absorption properties. In our study, we report the synthesis of two new fluorescent two-photon absorbing octupolar compounds that can be described as $D(-\pi-A)_3$ systems, constituted of three push-pull branches, where D is an electron donor, π a conjugated system and A an electron acceptor (**Figure 1**).[9] The intrinsic TPA of those materials is resulting from intramolecular charge transfer (ICT) from triphenylamine donor core to strongly electron-withdrawing sulfone-based peripheral groups. In addition, phenylene-vinylene conjugated linkers allow efficient electron communication between the electro-active groups.[10] Branching leads to cooperative enhancement of the TPA properties, in relation with coherent excitonic coupling between the branches.[11] In particular, triphenylamine-based derivatives have been extensively reported these last years for several research fields, including solar cells, solid-state luminescence, and fluorescence probing for environmental and biological applications.[12, 13] At the molecular level, their branches are easily modifiable to perform further functionalization and obtain innovative materials, particularly suited for sensing and imaging bioapplications.[14-16] Thus, this family of octupolar fluorophores hold great potential for theranostics as it displays high TPA cross-sections in the biological window (700-900 nm) and almost no toxicity in human embryonic kidney 293 cells.[17]

However, the direct use of fluorophores in biological media is often limited by their poor photophysical properties and low solubility in water and part of organic solvents. In contrast, the strategy of building photoactive organic-inorganic hybrid materials by sol-gel process has already shown its efficiency in solving those issues while keeping a right balance between biocompatibility and performance for biomedical applications.[8] In particular, type II hybrid nanoparticles (NPs) can be obtained through surface functionalization of the organic compounds or by copolymerization of silylated fluorophores and silica precursors, where at least one fraction of the organic and inorganic components is linked through strong Si-C(sp^3) bonds. These fluorescent organosilica NPs have very interesting characteristics that make them

promising systems for different optical applications with lower toxicity, biocompatibility, and stability.

In this context, the aim of this work was to prepare novel two-photon-responsive triphenylamine-based molecules and to further integrate them in type II hybrid organosilica NPs using only organoalkoxysilane sources during the synthesis. Hence, fluorophores (F and F2) bearing hydroxyl-ending groups and respectively possessing one or two phenylene-vinylene linkers were synthesized, and their photophysical properties were investigated. Moreover, one of the two fluorophores was successfully trisilylated with isocyanatopropyltriethoxysilane and integrated in the sol-gel synthesis of fluorophore-based periodic mesoporous organosilica nanoparticles (PMO NPs). Two-photon excited fluorescence (TPEF) experiments were then performed to assess the bio-imaging potential of the resulting nanoparticles.

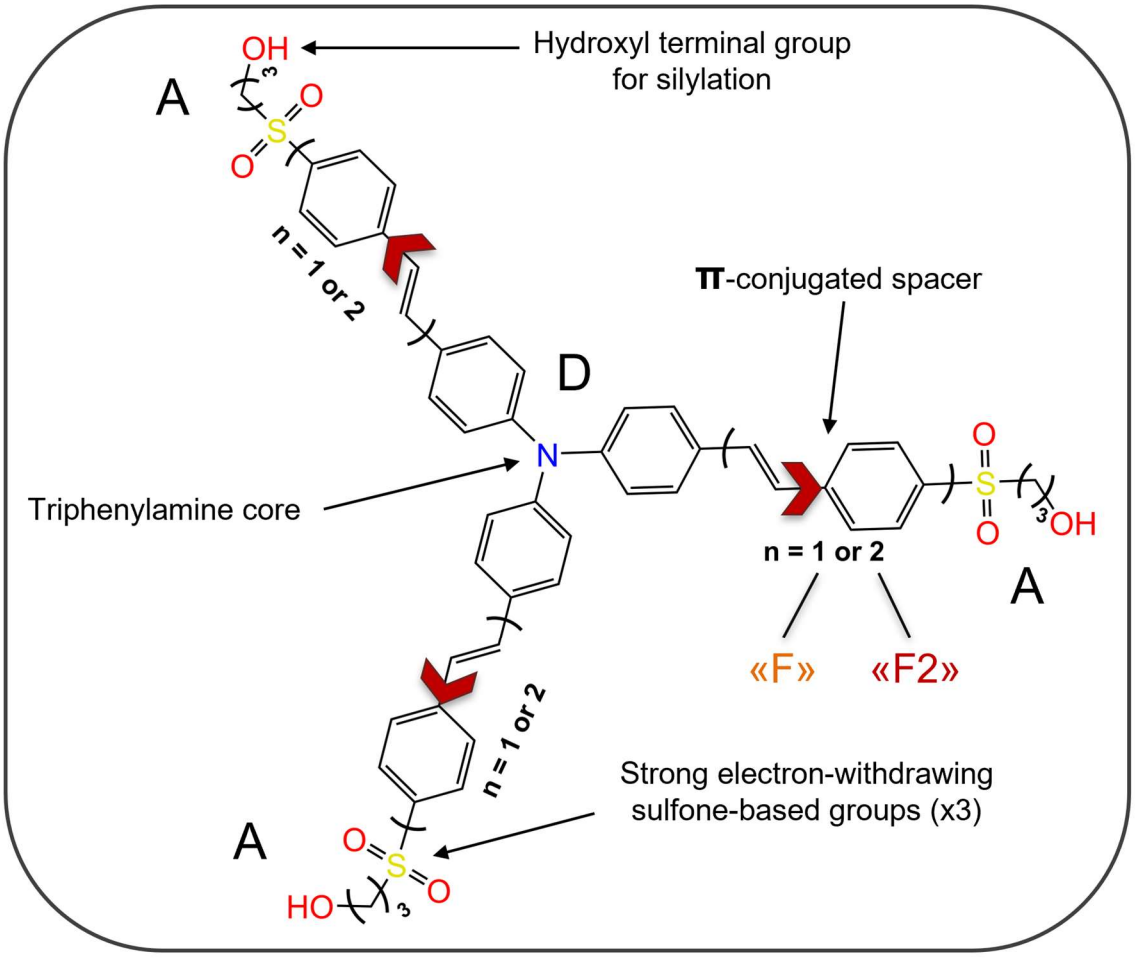

Figure 1. Structure and features of new two-photon responsive three-branched fluorophores F and F2. F and F2 are respectively composed of one and two phenylene-vinylene spacers. A: acceptor; D: donor.

2. Synthesis of new two-photon responsive fluorophores

The tripodal fluorophores F and F2 can basically be obtained by Heck reaction. This palladium-catalyzed vinylation takes place between an unsaturated halogen derivative and an alkene in the presence of a base, generally triethylamine, potassium carbonate or sodium acetate.[18-20] In our case, triphenylamine cores and sulfonyl-based branches were modified to bear either a halogen or alkene function for a final coupling yielding fluorescent products. All new molecules were fully characterized by NMR spectroscopy (^{1}H and ^{13}C), high-resolution mass spectrometry (HRMS) and elemental analysis to confirm their purity.

Firstly, triphenylamine moieties were uniformly modified in para positions (**Scheme 1**). Compound **1a** was obtained by a two-step trisformylation in Vilsmeier-Haack conditions *via* the bisaldehyde compound to allow higher yield for the third substitution.[21] Then, trisalkene **2** was formed by classic Wittig reaction with methyltriphenylphosphonium iodide.[17] In another process pathway, tris(4-iodophenyl)amine **1b** was produced in acidic medium by an adapted procedure.[22]

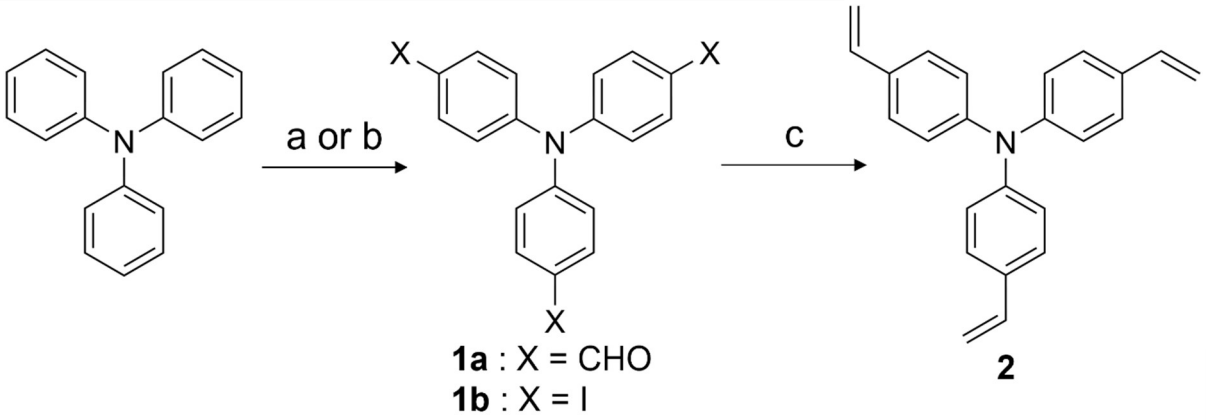

Scheme 1. Reagents and conditions for the preparation of triphenylamine-based cores. (a) Triphenylamine, $POCl_3$ (25 eq.), DMF (23 eq.), 95 °C, 4 h, then $POCl_3$ (50 eq.), DMF (49 eq.), 95 °C, 2h (41% of **1a**); (b) Triphenylamine, KI, HIO_4, acetic acid, 85 °C, 14 h (65% of **1b**); (c) **1a**, methyltriphenylphosphonium iodide, NaH, THF, 20 °C, 15 h (94% of **2**).

Secondly, after alkylation of 4-bromothiophenol with 3-bromopropanol, the resulting thioether **3** was oxidized by *m*-CPBA to reach the corresponding sulfone **4** (**Scheme 2**).[23] Then, Heck coupling between **4** and *p*-vinylbenzaldehyde **5**[24] under Jeffery's conditions using tetrabutylammonium bromide salt granted better reactivity and selectivity with 43% yield of intermediate compound **6**.[25]

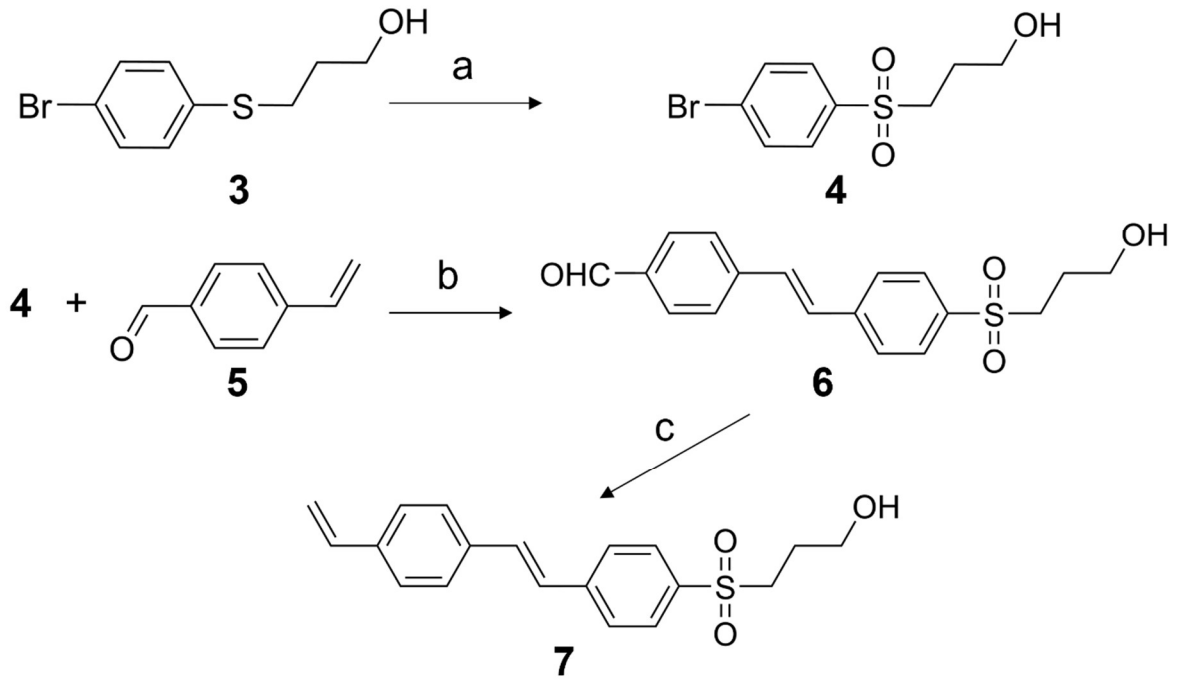

Scheme 2. Reagents and conditions for the preparation of branches with hydroxyl-ending group. (a) *m*-CPBA, DCM, 20 °C, 15 h (79% of **4**); (b) **4** (1.00 eq.), **5** (1.45 eq.), $Pd(OAc)_2$, PPh_3, K_2CO_3, *n*-Bu_4NBr, DMF, 90 °C, 20 h (43% of **6**); (c) methyltriphenylphosphonium iodide, *t*-BuOK, DCM, 20 °C, 15 h (13% of **7**).

The proton NMR spectrum in **Figure S1** confirmed the presence of aldehyde function with a singlet signal at δ = 10.05 ppm, and signal integration showed good correlation with the different equivalent protons in the structure. Intermediate **6** was then condensed with methyltriphenylphosphonium iodide to afford the vinyl product **7** with *E* stereochemistry, in pure and isolated form, as confirmed by ^{1}H NMR (**Figure S2**). The reaction yielded only 13% of distyrene derivative as $OPPh_3$ by-product presented similar polarity and solubility than **7** in the different solvent mixtures and chromatographic conditions tested.

Finally, treatment of trivinyl core **2** with brominated derivative **4** by classic Heck reaction afforded octupole **8**, namely fluorophore F (**Scheme 3**). Conversely, fluorophore **9** (F2) bearing an extended spacer with two phenylene-vinylene units was obtained under Jeffery's conditions by condensing triiodinated triphenylamine **1b** with the vinyl intermediate **7**. The two dyes exclusively presented *E* stereochemistry. Olefinic protons visible on NMR spectra were all detected at higher chemical shifts than if they were displaying a *Z* stereochemistry (**Figure S3, Figure S4**). In addition, the vicinal $^3J_{HH}$ coupling constants of all doublets were around 16.4 Hz (Experimental Section), which is characteristic of *trans* configuration.[26]

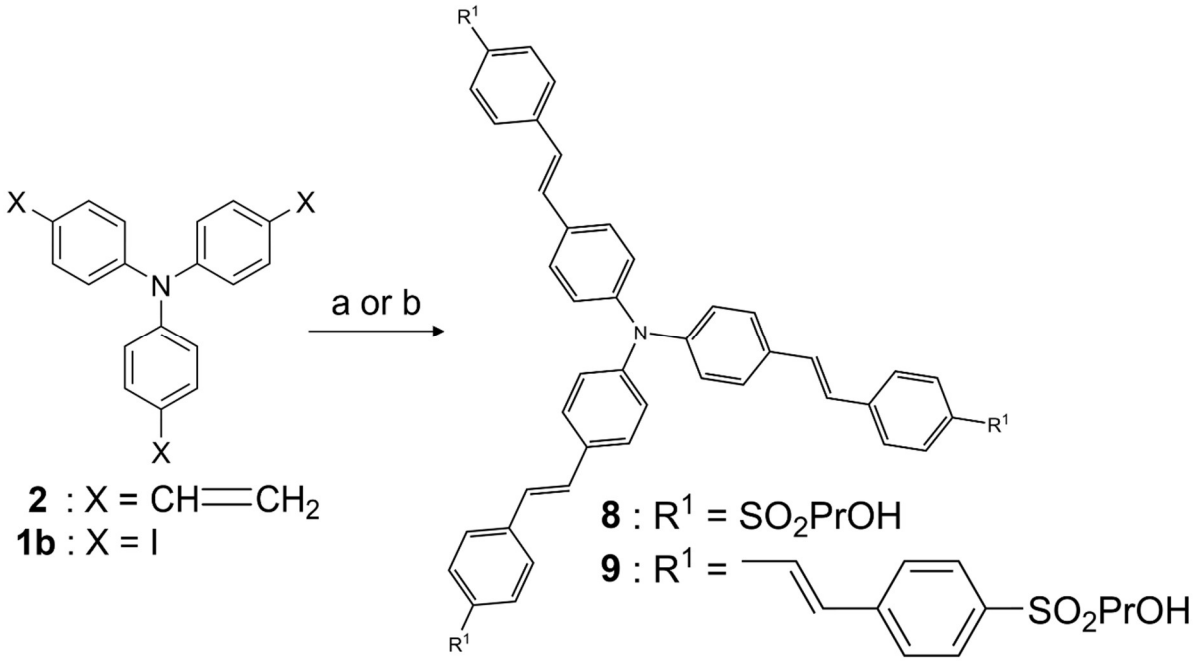

Scheme 3. Reagents and conditions for the preparation of three-branched fluorophores F (compound **8**) and F2 (compound **9**). (a) **2** (1.00 eq.), **4** (3.50 eq.), $Pd(OAc)_2$, $(o\text{-Tol})_3P$, Et_3N, DMF, 100 °C, 4 h (31% of **8**); (b) **1b** (1.00 eq.), **7** (4.50 eq.), $Pd(OAc)_2$, PPh_3, K_2CO_3, *n*-Bu_4NBr, DMF, 90 °C, 16 h (26% of **9**).

3. Photophysical studies of synthesized fluorophores

3.1 Photophysical characterizations

The photophysical properties of fluorophores F (**8**) and F2 (**9**) were first studied upon one-photon excitation. Solvent effects on absorbance and fluorescence of the octupoles were investigated in EtOAc, THF, DCM, EtOH, CH_3CN and DMSO. Due to their three alcohol functions, both compounds were insoluble in solvents of low polarity, such as toluene and pentane.

When increasing the solvent polarity, a strong bathochromic shift of the fluorescence emission band is observed, whereas little or no shift of the absorption band is detected (**Figure 2a-b**). Consequently, Stokes shift $\Delta\lambda$ ($\Delta\bar{\nu}$) values are increased and emission bands are remarkably broadened with increasing polarity, from 93 to 160 nm (4431 to 6904 cm^{-1}) and from 106 to 217 nm (4657 to 8143 cm^{-1}) half-bandwidths in the case of F and F2, respectively (**Table 1**). This effect is characteristic of ICT mechanism taking place upon excitation with fluorescence emission originating from a relaxed excited state localized on of the dipolar branches. This phenomenon is particularly interesting when $\Delta\lambda \geq 80$ nm for biological applications such as TPEF imaging, because of the variability of biological media polarities.[10, 17, 27, 28] For instance, such probes could serve in biodistribution studies or localization of materials used in theranostics.

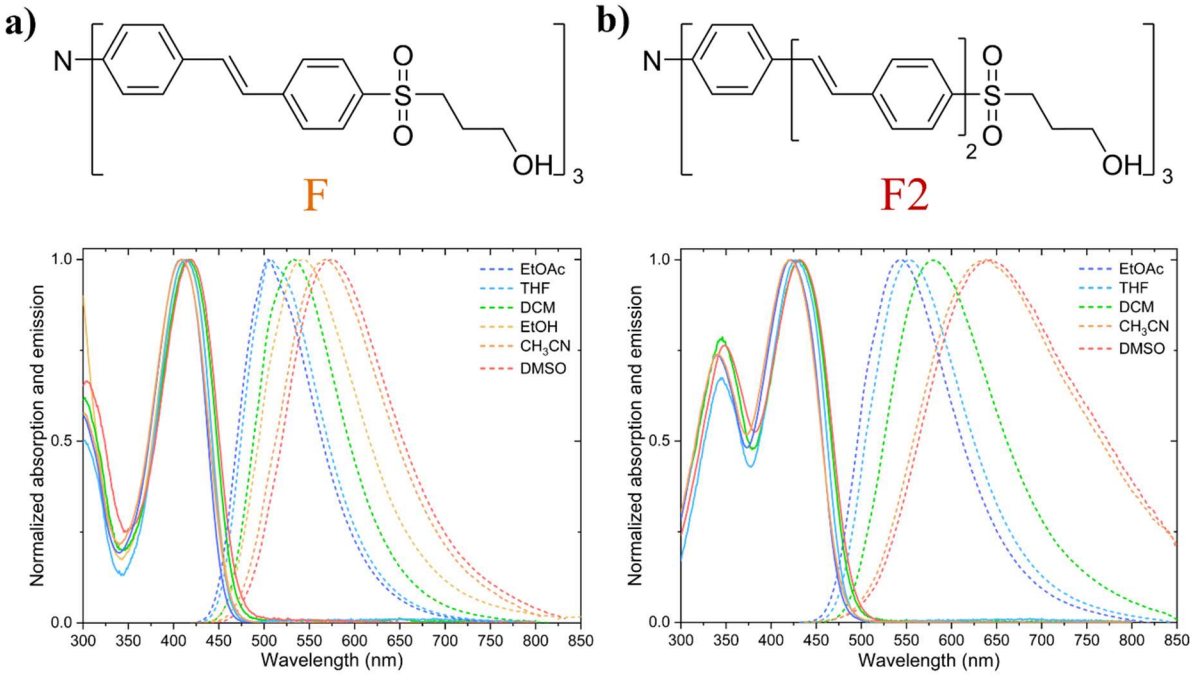

Figure 2. Normalized absorption and emission spectra of fluorophores (a) F and (b) F2. Increased solvent polarity induces the bathochromic shift of fluorescence emission.

As shown in **Table 1**, the fluorescence quantum yields decrease when the solvent polarity increases, due to fluorophore-solvent interactions, especially dipolar interactions of the fluorophore with its microenvironment. This decrease is sharper with extended compound F2.

Table 1. Solvatochromic data of octupolar chromophores F and F2. [a-b] Maximum absorbance (used for excitation) and emission wavelengths measured in solvents of various polarity. [c] Stokes shift ($1/\lambda_{abs.} - 1/\lambda_{em.}$). [d] Fluorescence quantum yields obtained using quinine bisulfate (QBS) in 0.5 M H_2SO_4 as a standard ($\Phi_{QBS} = 0.546$).

Name	Solvent	$\lambda_{abs.,\,max}$ [a] (nm)	$\lambda_{em.,\,max}$ [b] (nm)	$\Delta\bar{\nu}$ [c] (cm^{-1})	Φ_f [d]
F	EtOAc	408	504	4609	0.63
	THF	414	507	4431	0.65
	DCM	417	533	5219	0.63
	EtOH	411	544	5949	0.44
	CH_3CN	408	568	6904	0.32
	DMSO	420	575	6418	0.35
F2	EtOAc	422	542	5246	0.76
	THF	427	533	4657	0.75
	DCM	431	579	5931	0.70
	CH_3CN	419	636	8143	0.04
	DMSO	435	639	7339	0.06

Now comparing F and F2, the longer conjugated system of F2 presents significantly red-shifted absorption and emission bands, as well as an increase in fluorescence quantum yield in THF and DCM. F and F2 exhibit molar extinction coefficients in DCM of $\varepsilon_{max} = 8.1 \times 10^4$ and ε_{max}

= 1.1 × 10^5 M^{-1} cm^{-1}, respectively. Hence, the insertion of more phenylene-vinylene units also improves the brightness ($B = \varepsilon_{max} \Phi_f$) of the longest fluorophore (in DCM: B_F = 5.1 × 10^4 M^{-1} cm^{-1}; B_{F2} = 7.5 × 10^4 M^{-1} cm^{-1}).

3.2 Time-resolved fluorescence

Fluorescence lifetimes were determined in THF by using time-correlated single-photon counting. Both compounds displayed monoexponential fluorescence decays. F2 lifetime was found to be slightly shorter than that of F (2.2 and 2.5 ns, respectively, **Table 2**). These lifetimes are slightly higher than those measured for related octupolar compounds (1.0-1.9 ns). The radiative decay rate (k_r) of F2 is higher than that of F, in line with its extended π-system, whereas their non-radiative decay rates (k_{nr}) are quite similar, meaning that both compounds exhibit similar rigidity.

Table 2. Photophysical properties of chromophores F and F2 in THF. [a] Experimental fluorescence lifetimes and corresponding radiative ($k_r = \Phi / \tau$) and non-radiative ($k_{nr} = (1-\Phi) / \tau$) decay rates.

Name	Connector	Solvent	Φ_f	τ^a (ns)	k_r (10^9 s^{-1})	k_{nr} (10^9 s^{-1})
F	PV	THF	0.65	2.5	0.26	0.14
F2	PV_2	THF	0.75	2.2	0.34	0.11

3.3 Two-photon absorption properties

The two-photon absorption cross-sections (σ_2) of the two chromophores in the near infrared were measured by investigating their two-photon excited fluorescence (TPEF) properties. A fully quadratic dependence of the fluorescence intensity on the irradiation power (*i.e.* a linear dependence of the fluorescence intensity on the square of the irradiation power) was observed for each chromophore, showing that the obtained values are only due to TPA (**Figure S16**). Both compounds exhibit a strong TPA response in the biological window. The maximum TPA cross-section of the short compound F is the same as that of the extended one F2 (810 GM), but at a shorter wavelength (700 nm *vs.* 760 nm). Extension of the π-conjugated system of F2 leads to a red-shift and a broadening of the TPA band: F exhibits a sharp peak between 700 and 750 nm and then a plateau with σ_2 ~ 250 GM up to 850 nm, whereas the TPA band of F2 is much broader, leading to cross-sections higher than 450 GM in the whole 700-850 nm range, which is well-suited for TPEF imaging (**Table 3 and Figure 3**).

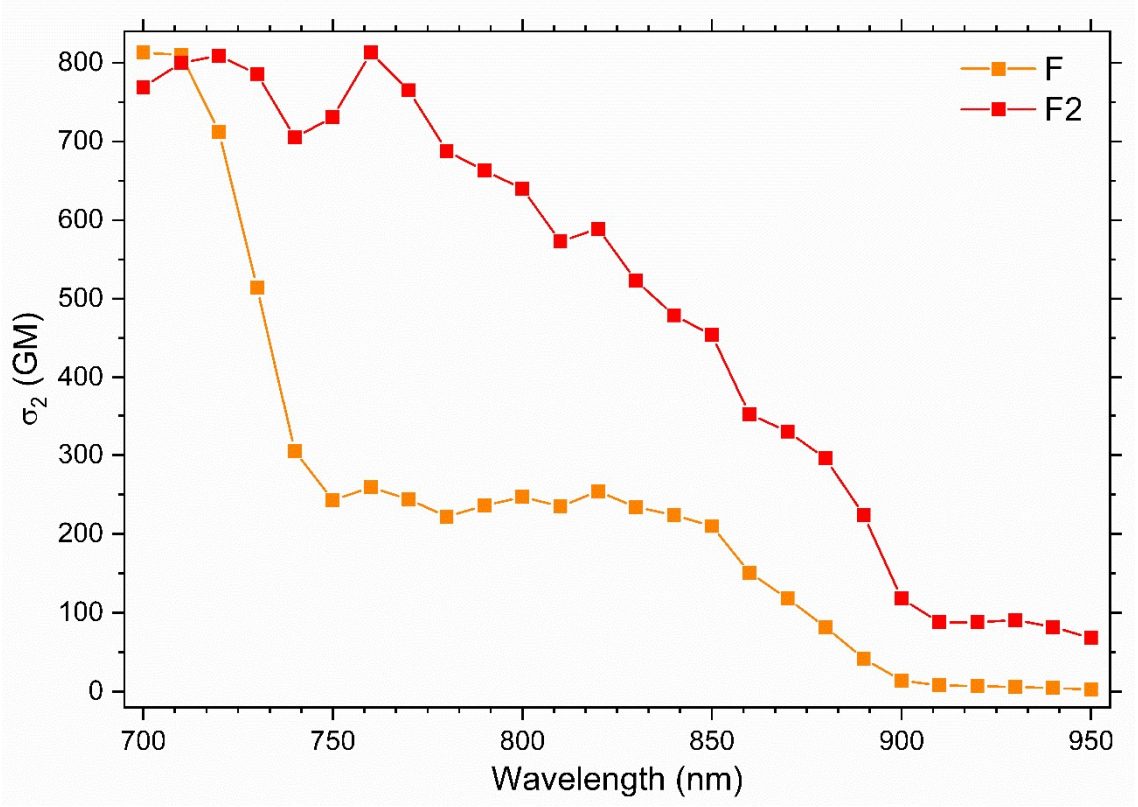

Figure 3. Two-photon absorption spectra of chromophores F and F2 in THF.

Table 3. Two-photon absorption properties of chromophores F and F2 in THF.

Name	Connector	$2\lambda^{abs}_{max}$ (nm)	λ^{TPA}_{max} (nm)	σ_{2max} (GM)
F	PV	822	700	810
F2	PV_2	854	760	810

4. Preparation of fluorophore-based PMO NPs

Following the synthesis and photophysical characterization of the fluorophores, an attempt was made to build fluorescent PMO nanoparticles with high potency for bio-imaging. To achieve this goal, we proposed to include two-photon chromophores directly in the PMO framework. Prior to the sol-gel process leading to the formation of organosilica nanoparticles, fluorophore F designed beforehand was silylated by condensation with isocyanatopropyltriethoxysilane (ICPTES) in the presence of triethylamine, following a workup adapted from previously reported procedures (**Figure 4a**).[29-31] Thus, hydroxyl-terminated F was trisilylated by formation of carbamate groups. The successful silylation of the so-called F-Si precursor was confirmed by ^{1}H NMR spectroscopy by a signal corresponding to the carbamate proton (H_9, relative ^{1}H ≈ 3) which appeared at δ = 6.26 ppm (**Figure S5**). It should be noted that only fluorophore F was chosen because it was soluble enough in the sol-

gel reaction medium. As a comparison, fluorophore F2 showed very limited solubility in polar protic solvents due to its longer conjugated arms.

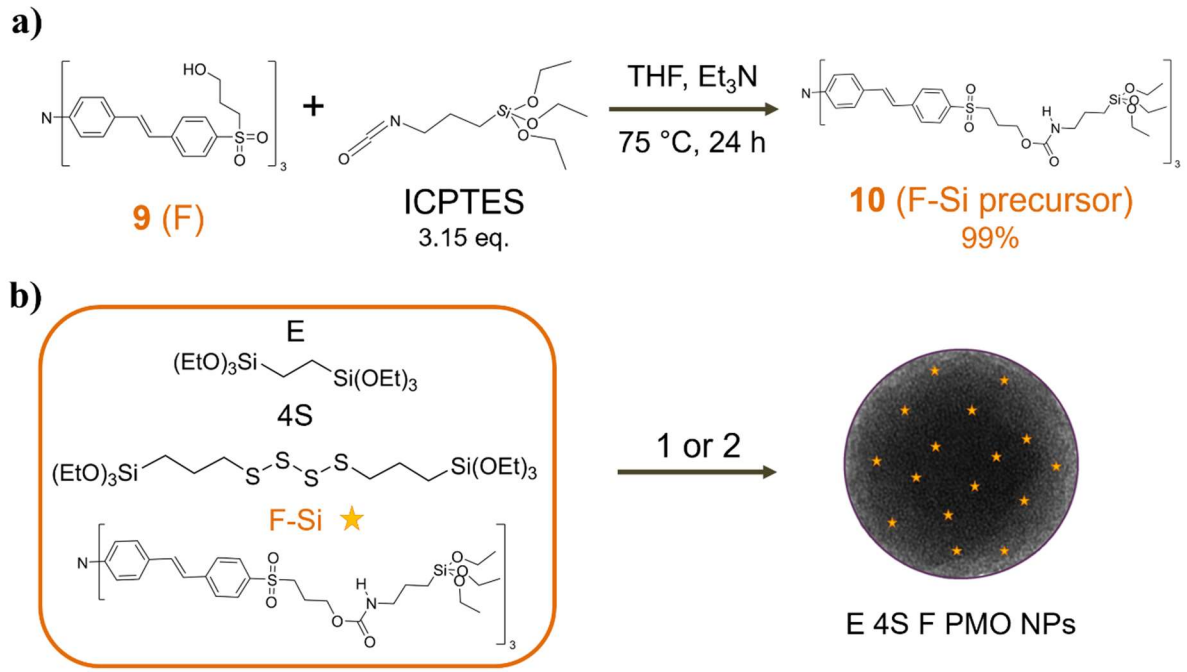

Figure 4. Preparation of fluorophore-based periodic mesoporous organosilica nanoparticles (F PMO NPs). (a) Silylation process of fluorophore F and (b) integration of resulting F-Si precursor in the sol-gel synthesis of E 4S F PMO NPs. (1) H_2O, EtOH, NaOH, CTAB, 80 °C, 2h; (2) H_2O, EtOH, NH_4OH, CTAB, 20 °C, 72 h in darkness. 4S: Bis[3-(triethoxysilyl)propyl]tetrasulfide; CTAB: Cetyltrimethylammonium bromide; E: 1,2-Bis(triethoxysilyl)ethane; ICPTES: 3-(Isocyanatopropyl)triethoxysilane.

The preparation of F PMO NPs was achieved under different sol-gel conditions using a basic catalyst to afford better control on the nanoparticle size dispersion. 1,2-bis(triethoxysilyl)ethane (E) and bis[3-(triethoxysilyl)propyl]tetrasulfide were employed as the main precursors, along with a slight fraction of F-Si (0.5%n, **Figure 4b**). Briefly, the syntheses of E 4S F-1a and E 4S F-1b were performed in aqueous medium for two hours with respectively low or high water and sodium hydroxide catalyst contents (**Figure 4b,** Route 1). E 4S F-2 NPs were obtained after three days of reaction and using ammonia as catalyst (**Figure 4b,** Route 2). In this procedure, a 2.6:1 (v:v) water:ethanol medium was employed to enhance F-Si solubility (**Table 4**).

Table 4. Synthesis conditions and size measurements of different E 4S F PMO NPs. [a] z average hydrodynamic diameter in ethanol, n = 5 independent experiments. [b] Average diameters of n ≥ 100 counts determined on TEM images. [c] Zeta potential measurement, n = 3 independent experiments (0.25 mM PBS). DLS: Dynamic light scattering; PDI: Polydispersity index; TEM: Transmission electronic microscopy.

PMO NPs	Catalyst	E:4S:F-Si:cat.:H_2O ratio (n:n)	DLS[a] (nm)	PDI	TEM[b] (nm)	ζ[c] (mV)
E 4S F-1a	NaOH	1:0.25:0.006:1.21:5049	383 ± 13	0.16 ± 0.10	171 ± 22	-24.3 ± 0.5
E 4S F-1b	NaOH	1:0.25:0.006:2.43:9326	275 ± 1	0.23 ± 0.05	143 ± 28	-29.0 ± 2.4
E 4S F-2	NH_4OH	1:0.11:0.006:0.33:1361	211 ± 2	0.07 ± 0.03	149 ± 26	-35.7 ± 0.6

Notably, according to dynamic light scattering measurements, E 4S F-2 NPs present a great monodispersity in size, with an average diameter of 211 ± 2 nm and a low polydispersity index (PDI) of 0.07 ± 0.03. In addition, transmission electronic microscopy imaging confirmed the sharp size distribution and revealed the formation of nanospheres (**Figure 5**), which can be associated with the composition of the reaction medium.

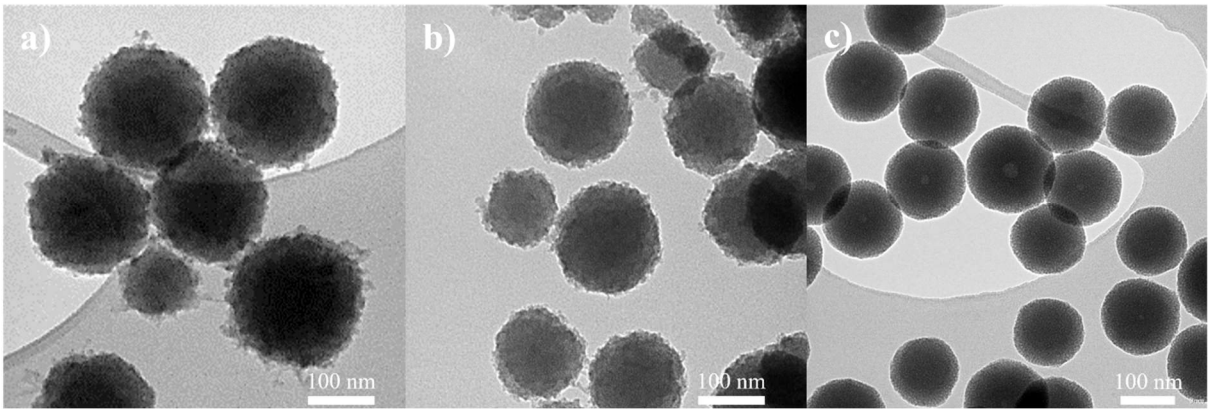

Figure 5. TEM imaging of synthesized fluorophore-based PMO NPs. Images of (a) E 4S F-1a, (b) E 4S F-1b, and (c) E 4S F-2 PMO NPs. Scale bar: 100 nm.

5. Applicability in two-photon fluorescence imaging

As-prepared F PMO NPs were tested as potent fluorescent markers to assess NPs internalization in cancer cells. To ensure their safety, cytotoxicity studies were performed on living breast cancer MCF-7 cells, revealing that the nanoparticles were biocompatible up to 100 µg mL^{-1} after three days of incubation with cells (**Figure S19**). Afterwards, confocal microscopy imaging of MCF-7 cells treated with 50 µg mL^{-1} of fluorophore-PMO for 24 h was performed (**Figure 6**). Results showed highly detectable cell internalization of fluorophore PMO NPs with higher efficiency for E 4S F-1b and E 4S F-2 than for E 4S F-1a. These observations were confirmed by the quantification of NPs inside the cancer cells performed

with ImageJ software (**Figure S20**). Hence, these results demonstrate the bio-imaging potential of fluorophore under two-photon excitation at 820 nm in the near-infrared region when the compound is integrated into various PMO frameworks.

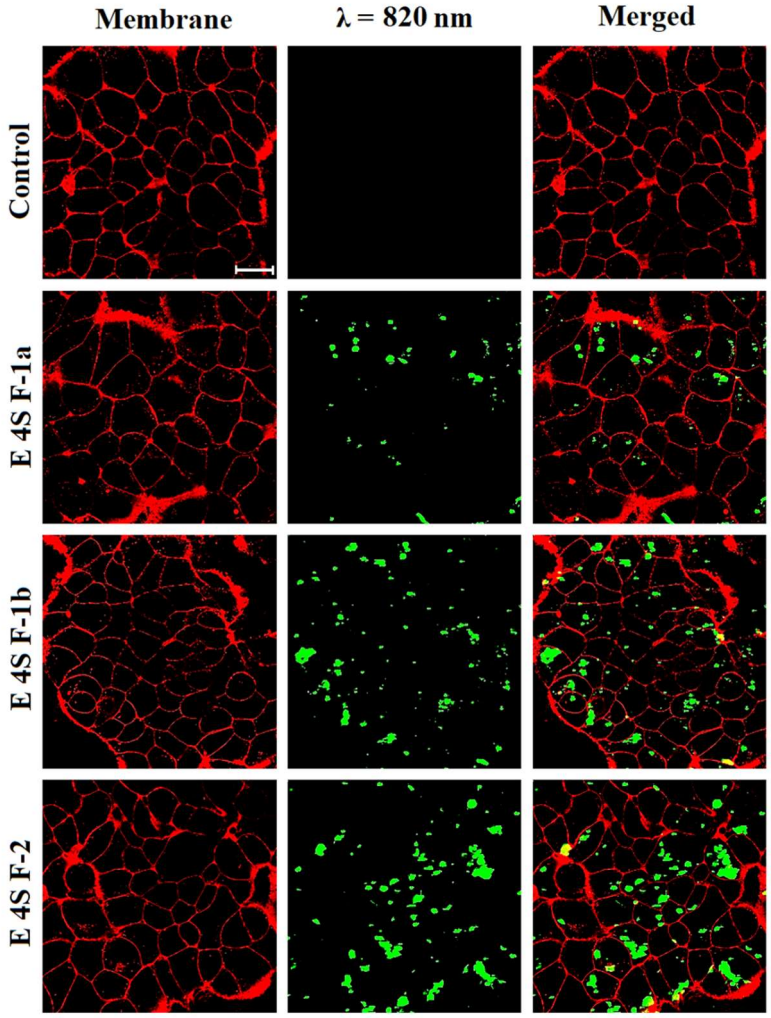

Figure 6. Cell internalization study of synthesized fluorophore-PMO NPs at 50 µg mL^{-1} using confocal microscopy imaging. MCF-7 cancer cells were stained with Cell Mask™ Orange Plasma Membrane after incubation for 24 h and then visualized at 561 nm (membrane) and 820 nm (F PMO NPs). Images were obtained with Carl Zeiss LSM780 confocal fluorescence microscope using a high magnification (63×/1.4 OIL Plan-Apo). Scale bar: 20 µm.

6. Conclusions and perspectives

In conclusion, two new octupolar three-branched TPA fluorophores possessing a triphenylamine core were synthesized by multistep synthesis involving Heck coupling strategies. They revealed similar structure-property relationships than other trigonal $A(–\pi–D)_3$ and $D(–\pi–A)_3$ octupoles described in the literature, with strong influence of conjugation length and aromaticity, as well as dependence on donor and acceptor strengths.[32, 33]

F and F2 dyes are good candidates for bioapplications as they exhibit suitable photophysical properties in the near-infrared region, including tunable emission wavelength due to solvatochromic character, as well as high fluorescence quantum yield and TPA cross-sections values, thus allowing efficient intrinsic three-dimensional resolution.

Using the hydroxyl-pending groups, one of the newly synthesized fluorophores was successfully easily integrated in the synthesis of biocompatible organosilica nanoparticles, known to be particularly suited for a large scope of bioapplications. Considering the excellent two-photon absorption and fluorescence properties of the fluorophore moieties, they could serve as bio-imaging probes in combination with drug delivery. In addition, the high two-photon absorption cross-sections make them potential energy donors in strategies based on energy transfer, such as anticancer and antibacterial two-photon excited photodynamic therapy enhanced by Förster resonance energy transfer.

7. Experimental section

7.1 Materials

Unless otherwise specified, ACS reagent grade starting materials and solvents were used as received from commercial suppliers without further purification.

Deionized water (resistivity = 18.2 MΩ cm) obtained from an Aquadem™ system (Veolia Water Technologies, Saint-Maurice, France) was used in all experiments. 1,2-Bis(triethoxysilyl)ethane (E, 96%), bis[3-(triethoxysilyl)propyl]tetrasulfide (4S, ≥ 90%), cetyltrimethylammonium bromide (CTAB, > 98%) ammonium nitrate (NH_4NO_3, > 98%), 3-(isocyanatopropyl)triethoxysilane (ICPTES, 95%), dimethylformamide (DMF, distilled using CaH_2), dimethylsulfoxide (DMSO), tetrahydrofuran (THF, distilled using sodium-benzophenone), dichloromethane (DCM), ethyl acetate (EtOAc), diethyl ether (Et_2O), pentane, heptane, petroleum ether, acetonitrile (CH_3CN), sodium thiosulfate ($Na_2S_2O_3$), sodium bicarbonate ($NaHCO_3$), sodium sulfate (Na_2SO_4), magnesium sulfate ($MgSO_4$), palladium (II) acetate ($Pd(OAc)_2$), tri(*o*-tolyl)phosphine ((*o*-Tol)$_3$P), potassium carbonate (K_2CO_3), potassium iodide (KI, 99%), phosphate buffer solution (PBS, 1 M, pH 7.4), phosphoryl chloride ($POCl_3$, 99%), sodium hydroxide pellets (NaOH, ≥ 98%), sodium hydride (NaH, 60% dispersion in mineral oil), sulfuric acid (H_2SO_4), quinine bisulfate (QBS), 3-bromopropanol (97%), $CDCl_3$ (99.9 atom% D), acetone-*d*$_6$ ($(CD_3)_2CO$, 99.9 atom% D), THF-*d*$_8$ (99.9 atom% D) and 3-(4,5-dimethylthiazol-2-yl)-2,5-diphenyl tetrazolium bromide (MTT) were purchased from Merck (Saint-Quentin-Fallavier, France). Acetic acid, periodic acid (HIO_4), *m*-chloroperoxybenzoic

acid (*m*-CPBA, 70-75%), terephtalaldehyde (98%), potassium *tert*-butoxide (*t*-BuOK), 4-bromothiophenol (98%) tetrabutylammonium chloride (*n*-Bu_4Br), triphenylamine, methyltriphenylphosphonium iodide (≥ 98%), triphenylphosphine, triethylamine (Et_3N, > 99%) and fluorescein (laser grade 99%) were purchased from Thermo Fisher Scientific (Illkirch-Graffenstaden, France). Celite S® was obtained from VWR (Radnor, PA, USA). Silica for chromatography (0.04-0.63 mm silica gel, 60 Å pores, 40-60 µm) was purchased from Macherey-Nagel (Düren, Germany). Ammonia (28%), absolute ethanol (EtOH) and ethanol (96%) were obtained from Carlo Erba Reagents (Cornaredo, MI, Italy). Cell Mask™ Orange Plasma Membrane was obtained from Invitrogen (Cergy-Pontoise, France). Glass bottom 8-well tissue culture chambers were purchased from Sarstedt (Marnay, France).

7.2 Analytical techniques

^1H and ^{13}C NMR spectra were obtained with a Bruker Avance III (300 or 400 MHz) NMR spectrometer (Billerica, MA, USA). CHNS elemental analysis and high resolution mass spectrometry (HRMS) analyses were performed at the Centre Régional de Mesures Physiques de l'Ouest (C.R.M.P.O., Rennes, France) either with a Bruker MaXis 4G (ES^+, Methanol:DCM 90:10 (v:v)) or with a Bruker Ultraflex III (MALDI, DCTB matrix).

Melting points were determined using a Kofler bench (Wagner & Munz).

Samples for TEM measurements were deposited from suspensions on Cu Formvar/C holey grids and allowed to dry before observation. The main transmission electron microscopy (TEM) images were acquired using a JEOL 1200 EXII (Tokyo, Japan) operated at 120 kV. The quantification of the nanoparticles diameters was performed with the Image*J* software with at least 100 counts.

Hydrodynamic diameter and zeta potential measurements were recorded on Malvern NanoSeries (Malvern, UK) Zetasizer NanoZS (model ZEN3600) in a DTS1060C Zetacell (for the zeta potential) at 25 °C, with an equilibration time of 60 s and with automatic measurement, and data were treated by Zetasizer software using a Smoluchowski model.

7.3 Multistep synthesis of fluorophores

*Tris(4-formylphenyl)amine (**1a**)*

$POCl_3$ (28.6 mL, 305.72 mmol, 25 eq.) was added portionwise at 0 °C to anhydrous DMF (21.8 mL, 23 eq.). After 1h stirring, triphenylamine (3.00 g, 12.23 mmol, 1 eq.) was quickly added. The temperature was immediately shifted to 95 °C, and the reaction mixture was

stirred for 4h (solidification after 3-4h). Then, the reaction mixture was transferred to an ice bath and neutralized with 6M $NaOH_{aq.}$ solution. After addition of water, extractions in DCM, and drying over Na_2SO_4, the solvent was evaporated. The crude product was purified by column chromatography (DCM, then DCM/EtOAc 95/5) and a brown oil was recovered (2.89 g, ^1H NMR (300.13 MHz, $CDCl_3$): 90-95% dialdehyde, 5-10% trialdehyde estimated). $POCl_3$ (44.8 mL, 479.5 mmol, 50 eq.) was added portionwise at 0 °C to anhydrous DMF (36.4 mL, 49 eq.). After 1h30 stirring, the intermediary product (2.89 g, 1 eq.) was quickly additioned. The temperature was immediately shifted to 95 °C, and the reaction mixture was stirred for 2h. After extractions and purification like before, **1a** was obtained as a yellow solid (1.20 g, 41%). M.p. 233-235 °C; ^1H NMR (300.13 MHz, $CDCl_3$): δ=9.94 (s, 3H), 7.84 and 7.25 ppm (AA'XX', *J*=8.5 Hz, 12H).

*Tris(4-iodophenyl)amine (**1b**)*

Air was removed from a solution of triphenylamine (4.04 g, 16.47 mmol, 1.00 eq.) and acetic acid (60 mL) by blowing argon for 10 min. Then, KI (5.45 g, 32.83 mmol, 2.00 eq.) was added, followed by HIO_4 (3.50 g, 15.35 mmol, 0.93 eq.). The reaction mixture was heated at 85 °C for 14h. After evaporation of acetic acid, the solid was dissolved in DCM and consecutively washed with $Na_2S_2O_3$ and $NaHCO_3$. After drying over Na_2SO_4, the solvent was evaporated. Pure compound **1b** was obtained after recrystallization from CH_3CN and filtration, as a brown solid (6.47 g, 65%). ^1H NMR (300.13 MHz, $CDCl_3$): δ=7.53 and 6.81 ppm (AA'XX', *J*=8.8 Hz, 12H); ^{13}C NMR (75.47 MHz, $CDCl_3$): δ 146.8, 138.6, 126.2, 86.7 ppm.

*Tris(4-ethenylphenyl)amine (**2**)*

Air was removed from a solution of **1a** (400 mg, 1.21 mmol, 1.00 eq.) and $MePPh_3^+$, I^- (3.93 g, 9.72 mmol, 8.00 eq.) in anhydrous THF (9.1 mL, 93 eq.). Then, NaH (291 mg, 12.15 mmol, 10.00 eq.) was added and the reaction mixture was stirred at 20 °C for 24h. The excess of NaH was destroyed with ice at 0 °C. After addition of water, extractions with DCM, and drying over Na_2SO_4, the solvents were evaporated under reduced pressure. The crude product was purified by column chromatography (heptane/DCM, 40/60) and **2** was obtained a pale-yellow solid (370 mg, 94%). ^1H NMR (300.13 MHz, $CDCl_3$): δ=7.35 and 7.09 (AA'XX', *J*=8.7 Hz, 12 H), 6.72 (dd, *J*=17.6 Hz, *J*=10.9 Hz, 3H), 5.70 (dd, *J*=17.6 Hz, *J*=0.7 Hz, 3H), 5.22 ppm (dd, *J*=10.9 Hz, *J*=0.7 Hz, 3H).

*3-[(4-Bromophenyl)thio]propanol (**3**)*

Air was removed from a solution of NaH (4.68 g, 60% in mineral oil, 117 mmol, 2.21 eq.) in anhydrous DMF (31.7 mL). Then, 4-bromothiophenol (10 g, 52.9 mmol, 1.00 eq.) in anhydrous DMF (10.7 mL) was added dropwise to the solution *via* a dropping funnel at 0 °C (1h). After cooling to 20 °C, 3-bromopropanol was added. The reaction mixture was stirred overnight. After addition of water, extractions with EtOAc and drying over Na_2SO_4, the solvents were evaporated. The crude product was then purified by column chromatography (heptane/EtOAc, 70/30) to afford product **3** (8.83 g, 68%) as a pale-yellow oil. ^{1}H NMR (300.13 MHz, $CDCl_3$): δ=7.40 (d, *J*=8.4 Hz, 2H), 7.21 (d, *J*=8.4 Hz, 2H), 3.57 (q, *J*=5.6 Hz, 2H), 3.03 (t, *J*=7.1 Hz, 2H), 1.88 ppm (m, 2H).

*3-[(4-Bromophenyl)sulfonyl]propanol (**4**)*

Air was removed from a solution of **3** (8.83 g, 35.73 mmol, 1.00 eq.) in DCM (93 mL, 40 eq.). Then, *m*-CPBA (70-75%, 20.87 g, 84.67 mmol, 2.37 eq.) was added portionwise. The reaction mixture was stirred for 15h, and then neutralized with 50 mL of 5M $NaOH_{aq.}$ solution at 0 °C. After addition of water, extractions with DCM, and drying over $MgSO_4$, the solvent was evaporated. The crude product was purified by column chromatography (heptane/EtOAc, 50/50) to afford sulfone **4** (7.92 g, 79%) as a white solid. ^{1}H NMR (300.13 MHz, $CDCl_3$): δ=7.76 and 7.72 (AA'XX', *J*=8.7 Hz, 4H), 3.77 (t, *J*=5.9 Hz, 2H), 3.23 (t, *J*=7.8 Hz, 2H), 2.01 (m, 2H), 1.71 ppm (bs, 1H).

*p-Vinylbenzaldehyde (**5**)*

Air was removed from a solution of K_2CO_3 (7.73 g, 55.92 mmol, 1.25 eq.) and $MePPh_3^+$, Br^- (17.58 g, 49.21 mmol, 1.10 eq.) in anhydrous THF (65 mL, 18 eq.) by blowing argon for 20 min. Then, terephtalaldehyde (6.00 g, 44.73 mmol, 1.00 eq.) was added, and the reaction mixture was heated at 80 °C for 20h. After filtration through Celite S® with heptane, the solvent was evaporated. The residue was filtrated (heptane/EtOAc 90/10) and the solvent was evaporated. The crude product was purified by column chromatography (pentane, then pentane/EtOAc, 98/2 to 90/10) and **5** was obtained as a yellow oil (3.60 g, 61%). ^{1}H NMR (300.13 MHz, $CDCl_3$): δ=9.99 (s, 1H), 7.84 (d, *J*=8.3 Hz, 2H), 7.55 d, *J*=8.3 Hz, 2H), 6.77 (dd, *J*=17.6 Hz, *J*=10.9 Hz, 1H), 5.90 (d, *J*=17.6 Hz, 1H), 5.43 ppm (d, *J*=10.9 Hz, 1H).

*4-[(1E)-2-{4-[(3-Hydroxypropyl)sulfonyl]phenyl}ethenyl]benzaldehyde (**6**)*

Air was removed from a solution of **4** (800 mg, 2.87 mmol, 1.00 eq.) and **5** (549 mg, 4.16 mmol, 1.45 eq.) in anhydrous DMF (13.1 mL, 60 eq.) by blowing argon for 30 min. Then,

$Pd(OAc)_2$ (32.2 mg, 0.14 mmol, 0.05 eq.), PPh_3 (75.2 mg, 0.29 mmol, 0.10 eq.) and *n*-Bu_4NBr (924 mg, 2.87 mmol, 1.00 eq.) were added. The reaction mixture was heated at 90 °C for 20h. After addition of water, extractions with EtOAc, and drying over Na_2SO_4, the solvent was evaporated. The crude product was purified by solid deposit (DCM) column chromatography (heptane/EtOAc, 30/70 to 25/75) and **6** was obtained as a white solid (410 mg, 43%). M.p. 152-154 °C; ^1H NMR (300.13 MHz, $CDCl_3$): δ=10.05 (s, 1H), 7.95 (m, 4H), 7.73 (m, 4H), 7.29 (d, 2H), 3.79 (q, *J*=5.7 Hz, 2H), 3.29 (m, 2H), 2.04 (m, 2H), 1.61 ppm (t, *J*=5.3 Hz, 1H); ^{13}C NMR (75.47 MHz, $CDCl_3$): δ=191.4, 142.2, 142.0, 138.3, 136.1, 131.3, 130.3, 129.9, 128.7, 127.4, 127.4, 60.6, 53.4, 25.8 ppm; HRMS (ES^+, $CH_3OH/CHCl_2$, 90/10): m/z calcd for $C_{18}H_{18}O_4S$: 353.0818 $[M+Na]^+$; found: 353.0823 ; elemental analysis calcd (%) for $C_{18}H_{18}O_4S$ (330.09): C 65.43, H 5.49, S 9.70; found: C 65.36, H 5.44, S 9.43.

*1-Ethenyl-4-[(1E)-2-{4-[(3-hydroxypropyl)sulfonyl]phenyl}ethenyl]benzene (**7**)*

Air was removed from a solution of **6** (1.40 g, 4.24 mmol, 1.00 eq.) and $MePPh_3^+$, I^- (3.43 g, 8.47 mmol, 2.00 eq.) in anhydrous DCM (90 mL, 333 eq.) by blowing argon for 10 min. Then, *t*-BuOK (1.47 g, 13.14 mmol, 3.10 eq.) was added. The reaction mixture was stirred for 15h. After filtration through Celite S® with DCM, the solvent was evaporated. The crude product was purified by column chromatography (heptane/DCM, 50/50). Fractions containing the product were gathered and purified by solid deposit (DCM) column chromatography (DCM/EtOAc, 95/5 to 75/25) and the eluent was evaporated. Then, the residue was triturated with Et_2O, $OPPh_3$ by-product was removed and **7** was obtained as a pale-yellow solid (185 mg, 13%). M.p. 192-194 °C; ^1H NMR (300.13 MHz, $CDCl_3$): δ=7.92 (d, *J*=8.4 Hz, 2H), 7.69 (d, *J*=8.4 Hz, 2H), 7.53 (d, *J*=8.3 Hz, 2H), 7.46 (d, *J*=8.3 Hz, 2H), 7.26 (d, *J*=16.3 Hz, 1H) 7.15 (d, *J*=16.3 Hz, 1H), 6.76 (dd, *J*=17.6 Hz, *J*=10.9 Hz, 1H), 5.82 (d, *J*=17.6 Hz, 1H), 5.32 (d, *J*=10.9 Hz, 1H), 3.79 (q, *J*=5.7 Hz, 2H), 3.27 (m, 2H), 2.04 (m, 2H), 1.61 ppm (t, *J*=5.3 Hz, 1H); ^{13}C NMR (75.47 MHz, $CDCl_3$): δ=142.9, 138.0, 137.3, 136.3, 135.8, 132.3, 128.5, 127.2, 127.0, 126.7, 126.4, 114.5, 60.6, 53.4, 25.8 ppm; HRMS (ES^+, $CH_3OH/CHCl_2$, 90/10): m/z calcd for $C_{19}H_{20}O_3S$: 351.10254 $[M+Na]^+$; found: 351.1024; elemental analysis calcd (%) for $C_{19}H_{20}O_3S$ (328.11): C 69.49, H 6.14, S 9.76; found: C 68.86, H 5.74, S 9.85.

*Tris{4-[(1E)-2-{4-[(3-hydroxypropyl)sulfonyl]phenyl}ethenyl]phenyl}amine (**8**) – F*

Air was removed from a solution of **2** (400 mg, 1.24 mmol, 1.00 eq.) and **4** (1.21 g, 4.328 mmol, 3.50 eq.) in anhydrous DMF (11.5 mL, 120 eq.) and Et_3N (0.7 mL, 4.95 mmol, 4.00 eq.) by blowing argon for 20 min. Then, $Pd(OAc)_2$ (41.6 mg, 0.19 mmol, 0.15 eq.) and (*o*-

Tol)$_3$P (113 mg, 0.37 mmol, 0.30 eq.) were added. The reaction mixture was heated at 100 °C for 4h. After filtration through Celite S® with DCM, addition of water, extractions with DCM, and drying over $MgSO_4$, the solvents were evaporated. The crude product was purified by solid deposit (DCM) column chromatography (EtOAc/EtOH/Et_3N, 96/3/1 to 87/12/1) to afford fluorophore **8** (F) as an orange solid (349 mg, 31%). M.p. 146-148 °C; ^{1}H NMR (300.13 MHz, $(CD_3)_2CO$): δ=7.90 (d, *J*=8.6 Hz, 6H), 7.86 (d, *J*=8.6 Hz, 6H), 7.66 (d, *J*=8.6 Hz, 6H), 7.51 (d, *J*=16.4 Hz, 3H), 7.33 (d, *J*=16.4 Hz, 3H), 7.16 (d, *J*=8.6 Hz, 6H), 3.73 (m, 3H), 3.62 (q, *J*=5.8 Hz, 6H), 3.30 (m, 6H), 1.88 ppm (m, 6H) ; ^{13}C NMR (75.47 MHz, $(CD_3)_2CO$): δ=148.3, 144.0, 139.0, 133.1, 132.7, 129.5, 129.3, 127.8, 126.7, 125.3, 60.6, 54.0, 27.3 ppm; HRMS (ES^+, $CH_3OH/CHCl_2$, 90/10): m/z calcd for $C_{51}H_{51}NO_9S_3$: 940.26182 $[M+Na]^+$; found: 940.2622; elemental analysis calcd (%) for $C_{51}H_{51}NO_9S_3$ (917.27): C 57.39, H 2.57, N 1.49, S 10.21; found: C 57.19, H 2.78, N 1.39, S 10.22.

*Tris{4-[(1E)-2-(4{(1E)-2[4-(3-hydroxypropylsulfonyl)phenyl]ethenyl}phenyl]ethenyl]phenyl}amine (**9**) – F2*

Air was removed from a solution of **1b** (67.5 mg, 0.11 mmol, 1.00 eq.), **7** (160 mg, 0.49 mmol, 4.50 eq.) and K_2CO_3 (80.8 mg, 0.58 mmol, 5.40 eq.) in anhydrous DMF (5.0 mL, 596 eq.) by blowing argon for 30 min. Then, $Pd(OAc)_2$ (3.6 mg, 0.02 mmol, 0.15 eq.), PPh_3 (8.5 mg, 0.03 mmol, 0.30 eq.) and *n*-Bu_4NBr (157 mg, 0.49 mmol, 4.50 eq.) were added. The reaction mixture was heated at 90 °C for 16h. After solvent evaporation, the crude product was purified by solid deposit (DCM/EtOH) column chromatography (DCM/EtOH, 99/1 to 85/15). Fractions containing the product were gathered and purified by solid deposit (THF) column chromatography (petroleum ether/THF, 30/70 to 23/77) and the solvents were evaporated. Then, butylated hydroxytoluene impurity from THF was removed by recrystallization (pentane/Et_2O, then pentane/EtOH), to afford fluorophore **9** (F2) as a red solid (35.0 mg, 26%). M.p. 179-181 °C; ^{1}H NMR (300.13 MHz, THF-d_8): δ=7.87 (d, *J*=8.5 Hz, 6H), 7.76 (d, *J*=8.5 Hz, 6H), 7.57 (m, 12H), 7.51 (d, *J*=8.5 Hz, 6H), 7.40 (d, *J*=16.3 Hz, 3H), 7.29 (d, *J*=16.3 Hz, 3H), 7.24 (d, *J*=16.3 Hz, 3H), 7.13 (d, *J*=16.3 Hz, 3H), 7.11 (d, *J*=8.5 Hz, 6H), 3.68 (t, *J*=5.2 Hz, 3H), 3.52 (q, *J*=5.8 Hz, 6H), 3.18 (m, 6H), 1.81 ppm (m, 6H); ^{13}C NMR (75.47 MHz, THF-d_8): δ=147.9, 143.7, 139.7, 139.1, 136.9, 133.6, 132.8, 129.5, 129.3, 128.5, 128.2, 127.8, 127.7, 127.6, 127.4, 125.2, 60.6, 54.1, 27.4 ppm; HRMS (MALDI, DCTB): m/z calcd for $C_{75}H_{69}NO_9S_3$: 1223.4129 $[M^{+\cdot}]$; found: 1223.412.

*Tris{4-[(1E)-2-{4-[(3-{N-[3-(triethoxysilyl)propyl]carbamoyl}propyl)sulfonyl]phenyl}ethenyl]phenyl}amine (**10**) – F-Si*

Air was removed from a solution of fluorophore F (351.9 mg, 384 µmol, 1.00 eq.) and isocyanatopropyltriethoxysilane (299 µL, 1.21 mmol, 3.15 eq.) in anhydrous THF (2.6 mL, 31.5 mmol) and Et_3N (53.5 µL, 384 µmol, 1.00 eq.) in a sealed tube. The reaction mixture was heated at 75 °C for 24 h. After resolubilization in anhydrous THF, the solvent was evaporated to afford the silylated fluorophore **10** (F-Si) as a dark orange powder (632 mg, 99%). ^{1}H NMR (400 MHz, $(CD_3)_2CO$): δ=7.90 (d, *J*= 8.7 Hz, 6H), 7.87 (d, *J*= 8.7 Hz, 6H), 7.66 (d, *J*=8.7 Hz, 6H), 7.51 (d, *J*=16.4 Hz, 3H), 7.33 (d, *J*=16.4 Hz, 3H), 7.16 (d, *J*=8.7 Hz, 6H), 6.26 (t, *J*=6.4 Hz, 3H), 4.07 (t, *J*=6.3 Hz, 6H), 3.80 (q, *J*=7.0 Hz, 18H), 3.28 (m, 6H), 3.08 (q, *J*=6.6 Hz, 6H), 1.96 (m, 6H), 1.58 (m, 6H), 1.18 (t, *J*=7.0 Hz, 27H), 0.59 ppm (m, 6H); ^{13}C NMR (101 MHz, $(CD_3)_2CO$): δ=148.3, 144.2, 138.7, 133.1, 132.8, 129.6, 129.3, 127.9, 126.6, 125.3, 62.8, 59.0, 53.7, 44.4, 43.6, 25.0, 24.2, 18.9, 8.5 ppm; HRMS (ES^+, CH_3OH/CH_2Cl_2, 90/10): m/z calcd for $C_{81}H_{114}N_4O_{21}S_3Si_3$: 1681.63378 $[M+Na]^+$; found: 1681.6334.

7.4 Photophysical studies of synthesized fluorophores

Solvatochromism studies

All photophysical measurements were performed with freshly prepared air-equilibrated solutions of THF, DMSO, EtOH or DCM (HPLC grade) at 20 °C. The fluorophore samples used to prepare the solutions were freshly recrystallized or thoroughly washed with cooled ether/pentane prior to the measurements to remove any organic impurity. UV–Vis absorption spectra were recorded on dilute solutions (ca. 10^{-5} M) by using a Jasco V-770 spectrophotometer (Mary's Court Easton, MD, USA). One-photon excited steady-state fluorescence studies were performed in quartz cells of 1 cm path length using an Edinburgh Instruments FLS920 fluorimeter (Edinburgh, UK) in photon-counting mode or a Jasco FP-8300 fluorimeter (Mary's Court Easton, MD, USA). Fully corrected excitation and emission spectra were obtained on dilute solutions (ca. 10^{-6} M) with an optical density at $\lambda_{exc.} \leq 0.1$. The fluorescence quantum yield of each compound was calculated using the integral of the fully corrected emission spectra relative to that of a standard, quinine bisulfate (QBS, H_2SO_4 0.5 M, $\Phi_{QBS} = 0.546$).[34, 35]

Fluorescence lifetime

Fluorescence lifetimes were measured by time correlated single-photon counting (TCSPC) by using an Edinburgh Instrument (FLS920) fluorimeter. Excitation at 375 nm was achieved by a pulsed diode laser EPL-375. The Instrument Response Function (IRF, halfbandwidth ca. 1 ns) was measured at the excitation wavelength using a dilute colloidal silica suspension. The TCSPC traces were analyzed by standard iterative reconvolution methods implemented in the software of the fluorimeter.

Two-photon excited fluorescence experiments

TPEF experiments were performed using a femtosecond laser chain (Ti-Sapphire Chameleon Ultra II, Coherent with pulse picker, generating 100-130 fs pulses at a 5 MHz rate) and an Ocean optics QEPro CCD detector with integration times ranging from 100 ms to 10 s. The excitation beam crossed a lens before arriving on the sample and a 650 nm short-pass filter after the sample to remove the excitation signal and prevent damages on the CCD detector. The beam power was measured with a PMD100 console and a S142C integrating sphere sensor from Thorlabs. For emission intensity vs excitation power measurements, a λ/2 waveplate and a polarizer were used to vary the laser power. The two-photon excitation was recorded in solution, perpendicularly to the beam using an optical fiber connected to a CCD detector. To avoid inner filter effects related to the high dye concentrations used, the laser was focused on a corner of the cuvette. The quadratic dependence of the fluorescence intensity (I) on the irradiation power (P) (*i.e.* the linear dependence of I on P^2) was checked for each solution. Further, TPA cross-sections (σ_2) were determined from the TPEF cross-sections ($\sigma_2.\Phi_F$) and the absolute fluorescence emission quantum yield (Φ_F). The absolute quantum yields were measured with a C9920–03 Hamamatsu system. TPEF cross-sections of F and F2 solutions ([F] = 4.32 10^{-5} M in THF; [F2] = 3.30 10^{-5} M in THF) were measured relative to fluorescein (1.04 10^{-4} M in 0.01 M aqueous NaOH) using the well-established method described by Xu and Webb[36] and the appropriate solvent-related refractive index corrections.[37] Data points between 700 and 715 nm were corrected according to reference.[38] The experimental uncertainty on the TPA cross-sections is estimated to be ± 15%.

7.5 Synthesis of F PMO NPs

F PMO-1a

A mixture of CTAB (250 mg, 0.69 mmol), ultrapure water (65 mL), and sodium hydroxide (NaOH (2 M), 437 µL) was stirred at 80 °C for 50 min at 750 rpm in a 250 mL round bottom flask. Then, a mixture of 1,2-bis(triethoxysilyl)ethane, bis[3-

(triethoxysilyl)propyl]tetrasulfide (E:4S, 80:20 (n:n), total 0.90 mmol) and silylated fluorophore (F-Si, 7.5 mg, 4.5 µmol) in 1 mL of absolute ethanol was introduced in the reaction. The condensation process was conducted for 2 h. Then, the solution was cooled to 20 °C while stirring; fractions were gathered in propylene tubes and collected by centrifugation for 20 min at 20k rpm. Subsequently, the still surfactant-filled particles were solvent-extracted three times with ammonium nitrate solution (20 g L^{-1} ethanol) in order to remove the CTAB template, and washed three times with ethanol, water and ethanol. Each extraction and washing involved 20 min sonication at 40 °C and centrifugation for 15 min at 20k rpm. The nanoparticles were finally redispersed in ethanol and dried for a few hours under vacuum at 20 °C.

F PMO-1b

A mixture of CTAB (250 mg, 0.69 mmol), ultrapure water (120 mL), and sodium hydroxide (NaOH (2 M), 875 µL) was stirred at 80 °C for 50 min at 750 rpm in a 250 mL round bottom flask. Then, a mixture of 1,2-bis(triethoxysilyl)ethane, bis[3-(triethoxysilyl)propyl]tetrasulfide (E:4S, 80:20 (n:n), total 0.90 mmol) and silylated fluorophore (F-Si, 7.5 mg, 4.5 µmol) in 1 mL absolute ethanol was introduced in the reaction. The condensation process was conducted for 2 h. Then, the solution was cooled to 20 °C while stirring. NPs were extracted and washed according to the previously described protocol.

F PMO-2

A mixture of CTAB (242 mg, 0.66 mmol), ultrapure water (45 mL), absolute ethanol (15.5 mL) and ammonia (NH_4OH (2 M), 305 µL) was stirred at 20 °C for one hour at 750 rpm in a 250 mL round bottom flask. Then, a mixture of 1,2-bis(triethoxysilyl)ethane, bis[3-(triethoxysilyl)propyl]tetrasulfide (E:4S, 90:10 (n:n), total 2.06 mmol) and silylated fluorophore (F-Si, 19.5 mg, 11.8 µmol) in 2 mL absolute ethanol was introduced in the reaction. The condensation process was conducted for 72 h in the dark. NPs were extracted and washed according to the previously described protocol.

7.6 Biological studies

Cell line

Human breast adenocarcinoma cell line (MCF-7) was maintained in Dulbecco's Modified Eagle's Medium (DMEM/F12) supplemented with 10% fetal bovine serum (FBS) and 1% penicillin/streptomycin. Cells were allowed to grow in humidified atmosphere at 37°C under 5% CO_2.

Cytotoxicity study

MCF-7 cells were seeded in 96-well plates at a density of 2000 cells per well. Twenty-four hours after cell growth, cells were treated with different concentrations of E 4S F-1a, E 4S F-1b and E 4S F-2. Cells treated with the vehicle were considered as a control. After 3 days of incubation, cell viability was assessed by the colorimetric MTT (3-(4,5-dimethylthiazol-2-yl)-2,5-diphenyltetrazolium bromide) assay. Briefly, the assay principle is based on the ability of viable cells to reduce the yellow soluble tetrazolium compound into an insoluble formazan crystal. MTT was added to the cells to reach a final concentration of 0.5 mg mL^{-1}. After 4 h of incubation, the medium/MTT solution was aspirated and the formazan crystals were dissolved in EtOH/DMSO solution (1:1, (v:v)) with 20 min of shaking. The absorbance was measured at 540 nm and the percentage of cell viability was calculated according to the following equation: $(A_{test}/A_{control} \times 100)$.

Cell internalization study using confocal microscopy

MCF-7 cells were seeded in glass bottom 8-well tissue culture chambers. Twenty-four hours after seeding, cells were treated with 50 µg mL^{-1} of F PMO NPs for 24 h. Untreated cells were considered as a control. Fifteen minutes before the end of incubation, cells were treated with CellMask™ Orange Plasma membrane Stain (Invitrogen, USA) at a final concentration of 5 µg mL^{-1}. Cells were washed two times with culture medium before observation with confocal fluorescence microscope LSM780 (Carl Zeiss, France) at 820 nm for nanoparticles (TPEF) and 561 nm for CellMask™ Orange Plasma membrane stain, using a high magnification (63×/1.4 OIL Plan-Apo). The internalization level of nanoparticles inside MCF-7 cells was quantified using ImageJ software.

Declaration of competing interest

The authors declare that they have no known competing financial interests or personal relationships that could have appeared to influence the work reported in this paper.

Data availability

Data will be made available on request.

Acknowledgements

Agence Nationale de la Recherche: ANR-19-CE09-0034 (MSN-2hv) is gratefully acknowledged.

References and notes

(1) Caminade, A.-M.; Zibarov, A.; Cueto Diaz, E.; Hameau, A.; Klausen, M.; Moineau-Chane Ching, K.; Majoral, J.-P.; Verlhac, J.-B.; Mongin, O.; Blanchard-Desce, M. Fluorescent phosphorus dendrimers excited by two photons: synthesis, two-photon absorption properties and biological uses. *Beilstein Journal of Organic Chemistry* **2019**, *15*, 2287-2303. DOI: 10.3762/bjoc.15.221.

(2) Li, G.; Wang, S.; Yang, S.; Liu, G.; Hao, P.; Zheng, Y.; Long, G.; Li, D.; Zhang, Y.; Yang, W.; et al. Synthesis, Photophysical Properties and Two-Photon Absorption Study of Tetraazachrysene-based N-Heteroacenes. *Chemistry – An Asian Journal* **2019**, *14* (10), 1807-1813. DOI: 10.1002/asia.201801656.

(3) An, J. M.; Kim, S. H.; Kim, D. Recent advances in two-photon absorbing probes based on a functionalized dipolar naphthalene platform. *Organic & Biomolecular Chemistry* **2020**, *18* (23), 4288-4297. DOI: 10.1039/d0ob00515k.

(4) Feng, W.; Liu, K.; Zang, J.; Xu, J.; Peng, H.; Ding, L.; Liu, T.; Fang, Y. Resonance-Enhanced Two-Photon Absorption and Optical Power Limiting Properties of Three-Dimensional Perylene Bisimide Derivatives. *The Journal of Physical Chemistry B* **2021**, *125* (41), 11540-11547. DOI: 10.1021/acs.jpcb.1c07296.

(5) Pascal, S.; David, S.; Andraud, C.; Maury, O. Near-infrared dyes for two-photon absorption in the short-wavelength infrared: strategies towards optical power limiting. *Chemical Society Reviews* **2021**, *50* (11), 6613-6658. DOI: 10.1039/d0cs01221a.

(6) Wu, L.; Liu, J.; Li, P.; Tang, B.; James, T. D. Two-photon small-molecule fluorescence-based agents for sensing, imaging, and therapy within biological systems. *Chemical Society Reviews* **2021**, *50* (2), 702-734. DOI: 10.1039/d0cs00861c.

(7) Rouxel, C.; Charlot, M.; Mir, Y.; Frochot, C.; Mongin, O.; Blanchard-Desce, M. Banana-shaped biphotonic quadrupolar chromophores: from fluorophores to biphotonic photosensitizers. *New Journal of Chemistry* **2011**, *35* (9), 1771. DOI: 10.1039/c1nj20073a.

(8) Hu, L.; Zhang, G.; Liu, Y.; Guo, T.; Shao, L.; Ying, L. Efficient dendrimers based on naphthalene indenofluorene for two-photon fluorescent imaging in living cells and tissues. *Journal of Materials Chemistry C* **2020**, *8* (6), 2160-2170, 10.1039/C9TC05991A. DOI: 10.1039/C9TC05991A.

(9) Cvejn, D.; Michail, E.; Polyzos, I.; Almonasy, N.; Pytela, O.; Klikar, M.; Mikysek, T.; Giannetas, V.; Fakis, M.; Bureš, F. Modulation of (non)linear optical properties in tripodal molecules by variation of the peripheral cyano acceptor moieties and the π-spacer. *Journal of Materials Chemistry C* **2015**, *3* (28), 7345-7355. DOI: 10.1039/c5tc01293g.

(10) Katan, C.; Terenziani, F.; Mongin, O.; Werts, M. H. V.; Porrès, L.; Pons, T.; Mertz, J.; Tretiak, S.; Blanchard-Desce, M. Effects of (Multi)branching of Dipolar Chromophores on Photophysical Properties and Two-Photon Absorption. *The Journal of Physical Chemistry A* **2005**, *109* (13), 3024-3037. DOI: 10.1021/jp044193e.

(11) Xu, L.; Lin, W.; Huang, B.; Zhang, J.; Long, X.; Zhang, W.; Zhang, Q. The design strategies and applications for organic multi-branched two-photon absorption chromophores with novel cores and branches: a recent review. *Journal of Materials Chemistry C* **2021**, *9* (5), 1520-1536. DOI: 10.1039/d0tc05910b.

(12) Chen, S.; Chen, Q.; Luo, S.; Cao, X.; Yang, G.; Zeng, X.; Wang, Z. Progress in Design, Synthesis and Application of Triphenylamine-Based Fluorescent Probes. *Chinese Journal of Organic Chemistry* **2021**, *41* (3), 919. DOI: 10.6023/cjoc202009012.

(13) Gayathri, P.; Pannipara, M.; Al-Sehemi, A. G.; Anthony, S. P. Triphenylamine-based stimuli-responsive solid state fluorescent materials. *New Journal of Chemistry* **2020**, *44* (21), 8680-8696. DOI: 10.1039/d0nj00588f.

(14) Gopinath, A.; Manivannan, N.; Mandal, S.; Mathivanan, N.; Nasar, A. S. Substituent enhanced fluorescence properties of star alpha-cyanostilbenes and their application in bioimaging. *Journal of Materials Chemistry B* **2019**, *7* (39), 6010-6023. DOI: 10.1039/c9tb01452g.

(15) He, H. F.; Meng, X. Y.; Deng, L. L.; Sun, Q.; Huang, X. L.; Lan, N.; Zhao, F. A novel benzothiadiazole-based and NIR-emissive fluorescent sensor for detection of Hg(2+)and its application in living cell and zebrafish imaging. *Organic & Biomolecular Chemistry* **2020**, *18* (32), 6357-6363. DOI: 10.1039/d0ob01396j.

(16) Wen, X.; Yan, L.; Fan, Z. A novel AIE active NIR fluorophore based triphenylamine for sensing of Hg2+ and CN− and its multiple application. *Spectrochimica Acta Part A: Molecular and Biomolecular Spectroscopy* **2020**, *241*, 118664. DOI: https://doi.org/10.1016/j.saa.2020.118664.

(17) Le Droumaguet, C.; Sourdon, A.; Genin, E.; Mongin, O.; Blanchard-Desce, M. Two-Photon Polarity Probes Built from Octupolar Fluorophores: Synthesis, Structure-Properties Relationships, and Use in Cellular Imaging. *Chemistry - An Asian Journal* **2013**, *8* (12), 2984-3001. DOI: 10.1002/asia.201300735.

(18) Mizoroki, T.; Mori, K.; Ozaki, A. Arylation of Olefin with Aryl Iodide Catalyzed by Palladium. *Bulletin of the Chemical Society of Japan* **1971**, *44* (2), 581-581. DOI: 10.1246/bcsj.44.581 (acccessed 2022/07/19).

(19) Heck, R. F.; Nolley, J. P. Palladium-catalyzed vinylic hydrogen substitution reactions with aryl, benzyl, and styryl halides. *The Journal of Organic Chemistry* **1972**, *37* (14), 2320-2322. DOI: 10.1021/jo00979a024.

(20) Julia, M.; Duteil, M. Condensation of aromatic halides with olefins catalyzed by palladium(0). *Bulletin de la Société Chimique de France* **1973**, 2790.

(21) Mallegol, T.; Gmouh, S.; Meziane, M. A. A.; Blanchard-Desce, M.; Mongin, O. Practical and Efficient Synthesis of Tris(4-formylphenyl)amine, a Key Building Block in Materials Chemistry. *Synthesis* **2005**, *2005* (11), 1771-1774.

(22) Khanasa, T.; Jantasing, N.; Morada, S.; Leesakul, N.; Tarsang, R.; Namuangruk, S.; Kaewin, T.; Jungsuttiwong, S.; Sudyoadsuk, T.; Promarak, V. Synthesis and Characterization of 2D-D-π-A-Type Organic Dyes Bearing Bis(3,6-di-tert-butylcarbazol-9-ylphenyl)aniline as Donor Moiety for Dye-Sensitized Solar Cells. *European Journal of Organic Chemistry* **2013**, *2013* (13), 2608-2620. DOI: 10.1002/ejoc.201201479.

(23) Semple, G.; Santora, V. J.; Smith, J. M.; Covel, J. A.; Hayashi, R.; Gallardo, C.; Ibarra, J. B.; Schultz, J. A.; Park, D. M.; Estrada, S. A.; et al. Identification of biaryl sulfone derivatives as antagonists of the histamine H3 receptor: Discovery of (R)-1-(2-(4′-(3-methoxypropylsulfonyl)biphenyl-4-yl)ethyl)-2-methylpyrrolidine (APD916). *Bioorganic & Medicinal Chemistry Letters* **2012**, *22* (1), 71-75. DOI: https://doi.org/10.1016/j.bmcl.2011.11.075.

(24) Greenhalgh, M. D.; Frank, D. J.; Thomas, S. P. Iron-Catalysed Chemo-, Regio-, and Stereoselective Hydrosilylation of Alkenes and Alkynes using a Bench-Stable Iron(II) Pre-Catalyst. *Advanced Synthesis & Catalysis* **2014**, *356* (2-3), 584-590. DOI: 10.1002/adsc.201300827.

(25) Jeffery, T. On the efficiency of tetraalkylammonium salts in Heck type reactions. *Tetrahedron* **1996**, *52* (30), 10113-10130. DOI: https://doi.org/10.1016/0040-4020(96)00547-9.

(26) Fleming, I.; Williams, D. H. *Spectroscopic methods in organic chemistry*; Springer, 1966.

(27) Katan, C.; Charlot, M.; Mongin, O.; Le Droumaguet, C.; Jouikov, V.; Terenziani, F.; Badaeva, E.; Tretiak, S.; Blanchard-Desce, M. Simultaneous Control of Emission Localization and Two-Photon Absorption Efficiency in Dissymmetrical Chromophores. *The Journal of Physical Chemistry B* **2010**, *114* (9), 3152-3169. DOI: 10.1021/jp911445m.

(28) Gautam, P.; Wang, Y.; Zhang, G.; Sun, H.; Chan, J. M. W. Using the Negative Hyperconjugation Effect of Pentafluorosulfanyl Acceptors to Enhance Two-Photon Absorption in Push–Pull Chromophores. *Chemistry of Materials* **2018**, *30* (20), 7055-7066. DOI: 10.1021/acs.chemmater.8b02723.

(29) Biazzotto, J. C.; Sacco, H. C.; Ciuffi, K. J.; Ferreira, A. G.; Serra, O. A.; Iamamoto, Y. Synthesis and properties of urea porphyrinosilica. *Journal of Non-Crystalline Solids* **2000**, *273* (1), 186-192. DOI: https://doi.org/10.1016/S0022-3093(00)00167-8.

(30) Gary-Bobo, M.; Mir, Y.; Rouxel, C.; Brevet, D.; Basile, I.; Maynadier, M.; Vaillant, O.; Mongin, O.; Blanchard-Desce, M.; Morère, A.; et al. Mannose-Functionalized Mesoporous Silica Nanoparticles for Efficient Two-Photon Photodynamic Therapy of Solid Tumors. *Angewandte Chemie International Edition* **2011**, *50* (48), 11425-11429. DOI: 10.1002/anie.201104765.

(31) Lerouge, F.; Cerveau, G.; Corriu, R. J. P.; Stern, C.; Guilard, R. Self-organization of porphyrin units induced by magnetic field during sol–gel polymerization. *Chemical Communications* **2007**, (15), 1553-1555. DOI: 10.1039/b616421h.

(32) Tian, Y.-P.; Li, L.; Zhang, J.-Z.; Yang, J.-X.; Zhou, H.-P.; Wu, J.-Y.; Sun, P.-P.; Tao, L.-M.; Guo, Y.-H.; Wang, C.-K.; et al. Investigations and facile synthesis of a series of novel multi-functional two-

photon absorption materials. *Journal of Materials Chemistry* **2007**, *17* (34), 3646. DOI: 10.1039/b703853d.

(33) Chung, S.-J.; Kim, K.-S.; Lin, T.-C.; He, G. S.; Swiatkiewicz, J.; Prasad, P. N. Cooperative Enhancement of Two-Photon Absorption in Multi-branched Structures. *The Journal of Physical Chemistry B* **1999**, *103* (49), 10741-10745. DOI: 10.1021/jp992846z.

(34) Crosby, G. A.; Demas, J. N. Measurement of photoluminescence quantum yields. Review. *The Journal of Physical Chemistry* **1971**, *75* (8), 991-1024. DOI: 10.1021/j100678a001.

(35) Eaton, D. F. Reference materials for fluorescence measurement. *Pure and Applied Chemistry* **1988**, *60* (7), 1107-1114. DOI: doi:10.1351/pac198860071107.

(36) Xu, C.; Webb, W. W. Measurement of two-photon excitation cross sections of molecular fluorophores with data from 690 to 1050 nm. *J. Opt. Soc. Am. B* **1996**, *13* (3), 481-491. DOI: 10.1364/JOSAB.13.000481.

(37) Werts, M. H. V.; Nerambourg, N.; Pélégry, D.; Le Grand, Y.; Blanchard-Desce, M. Action cross sections of two-photon excited luminescence of some Eu(iii) and Tb(iii) complexes. *Photochemical & Photobiological Sciences* **2005**, *4* (7), 531-538. DOI: 10.1039/b504495b.

(38) Katan, C.; Tretiak, S.; Werts, M. H. V.; Bain, A. J.; Marsh, R. J.; Leonczek, N.; Nicolaou, N.; Badaeva, E.; Mongin, O.; Blanchard-Desce, M. Two-Photon Transitions in Quadrupolar and Branched Chromophores: Experiment and Theory. *The Journal of Physical Chemistry B* **2007**, *111* (32), 9468-9483. DOI: 10.1021/jp071069x.